Core-hole effect in the one-particle approximation revisited from density functional theory

Vincent Mauchamp* and Michel Jaouen
Laboratoire de Physique des Matériaux (PHYMAT), CNRS UMR 6630, SP2MI-Boulevard 3, Téléport 2-BP 30179, 86962 Futuroscope Chasseneuil Cedex, France

Peter Schattschneider
Institut for Solid States Physics, Vienna University of Technology, Wiedner Haupstraße 8-10, A-1040 Wien, Austria
(Received 17 February 2009; published 4 June 2009)

The strength of the core-hole effect in simulations of electron energy-loss near edge structures or x-ray absorption near edge structures is investigated using *ab initio* calculations based on the density functional theory. Calculations were performed using the WIEN2K and FEFF codes at different edges for the following model compounds: rutile TiO_2, MgO, and for some transition metals (Ti, Fe, Co, Cu, and Zn). We demonstrate that although a core hole is always present in any core-level spectroscopy experiment, its effect is not always observable. To observe or not a core-hole effect in any experimental situation can, however, be predicted from the examination of the material's ground-state electronic structure, especially of the states just above the Fermi level. Indeed, it is shown that the two important criteria governing the core-hole strength at a given edge depend first on the localization and on the character of the first empty states of the material under investigation, and second on the nature of the compensating charge necessary to maintain the crystal neutrality. These criteria are expected to give a good description of the core-hole effect in the one-particle approximation. However, nothing can be inferred as for the good/bad agreement between calculations and experiments for more complex cases such as excitations of delocalized semicore states or of atomiclike multiplet structures.

DOI: 10.1103/PhysRevB.79.235106 PACS number(s): 79.20.Uv, 78.70.Dm, 78.20.Bh, 77.84.Bw

I. INTRODUCTION

Fine structures observed on spectra obtained from electron energy-loss spectroscopy (EELS) (Ref. 1) or x-ray absorption spectroscopy (XAS) (Ref. 2) experiments can often be interpreted successfully thanks to well established theoretical methods.[3,4] For instance, first-principles calculations have been used for chemical bonding analysis,[5,6] for studying electronic structure anisotropy,[7,8] alloying effects,[9] or local distortions at interfaces.[10] In condensed-matter physics, such simulations are often performed by using electronic structure calculations based on the density functional theory (DFT).[11] Within this framework, the fundamental quantity, the charge density, is calculated from one-particle wave functions [the Kohn-Sham (KS) orbitals] obtained self-consistently through the calculation of a potential that includes all correlation effects occurring inside the solid. However, the DFT being a ground-state theory, one is always facing the problem of the impact of the core hole created during the excitation process on the electronic structure and thus on the so predicted fine structures.

In the nonrelativistic first Born approximation, and ignoring dynamical diffraction effects,[12] the inelastic-scattering EELS cross section is given by[13]

$$\sigma(\omega)_{\mathrm{EELS}} = \sigma_{\mathrm{Ru}} \int S(\mathbf{q},\omega) d\mathbf{q}, \tag{1}$$

where the index Ru refers to the electron-electron Rutherford scattering cross section. Despite being out of the scope of the present paper, note that Eq. (1) also describes nonresonant inelastic x-ray scattering (NRIXS) (Ref. 14) if we replace σ_{Ru} by the Thomson scattering cross section σ_{Th}. Therefore, EELS and NRIXS only differ by the coupling of the probe (EELS: electrons, NRIXS: photons) interacting with the system, but both carry the same information (see Ref. 15 and references therein).

The dynamical form (or structure) factor (DFF) $S(\mathbf{q},\omega)$ describes the excitation of the system from its initial state $|\Psi_i\rangle$ to the final states $|\Psi_f\rangle$. It is a function of the momentum transfer $\mathbf{q}$ and of the energy ω involved in the transition. If $|\Psi_i\rangle$ and $|\Psi_f\rangle$ are approximated to one-particle states, the DFF can be expressed in terms of the Fermi golden rule, e.g., a matrix element of a transition operator $\hat{A}$ between these two states. When considering a small momentum transfer, $\hat{A}$ can be expressed in terms of a dipole operator.[2,16] Using atomic units (a.u.), it is then given by

$$S(\mathbf{q},\omega) = \sum_f |\langle \Psi_i | \mathbf{q}\cdot\mathbf{r} | \Psi_f \rangle|^2 \delta(\omega - E_f + E_i). \tag{2}$$

Concerning XAS, using the above mentioned approximations, the absorption cross section can also be expressed in terms of the Fermi golden rule,[17]

$$\sigma(\omega)_{\mathrm{XAS}} = 4\pi^2 \alpha\omega \sum_f |\langle \Psi_i | \boldsymbol{\varepsilon}\cdot\mathbf{r} | \Psi_f \rangle|^2 \delta(\omega - E_f + E_i), \tag{3}$$

where $\boldsymbol{\varepsilon}$ is the electric field polarization vector and α the fine-structure constant. The momentum $\mathbf{q}$ in an EELS experiment playing the same role as the polarization vector $\boldsymbol{\varepsilon}$ in XAS, both spectroscopies can be interpreted using similar theories and give comparable results.[18,19] Within the previously mentioned approximations, electron energy-loss near edge structures (ELNES) or x-ray absorption near edge structures (XANES) spectra can be, to first order, correlated with the unoccupied density of states of the excited atom projected on the proper symmetries allowed by the dipole selection rules.[20] It is worth mentioning that this formalism is no longer valid when many-body effects (core hole photoelec-

tron interaction, local-field effects due to the screening of the incoming field) require to go beyond the one-particle approximation, i.e., when $|\Psi_i\rangle$ and $|\Psi_f\rangle$ are not one-particle states. These two-particle interactions need to be treated using other theoretical schemes such as the Bethe-Salpeter equation (BSE),[21] or a combined BSE-TDDFT (time-dependent DFT) approach.[22]

It follows from Eqs. (2) and (3) that the main task when modeling an experimental spectrum is the proper calculation of the KS orbitals $|\Psi_i\rangle$ and $|\Psi_f\rangle$; the important question is to know if one has to consider or not the contribution of the positive charge induced by the hole. Indeed, this perturbation can strongly modify the potential of the excited atom: the valence/conduction states can then be contracted and shifted in energy.[23] The projected density of states can thus change and the overall shape of the spectrum be strongly modified even leading to excitonic peaks in the ELNES or XANES. Such modifications are generally well reproduced by DFT calculations that explicitly include the core hole. This is illustrated by Moreau *et al.* in the case of the carbon *K* edge in lamellar C_3N_4 compounds,[24] Jaouen *et al.* for the simulation of the boron *K* edge in hexagonal boron nitride[25] or Jiang *et al.* when calculating the lithium and oxygen *K* edges in Li_2O.[26]

It is often believed that in insulators and semiconductors, the core hole should be systematically included into the calculation since the valence electrons do not have the freedom to screen it.[4] This is confirmed by studies of Li_2O, Si, MgO, or SiO_2 where the systematic inclusion of the core-hole effect is necessary to reach satisfactory agreement with the experimental spectra.[26,27] Counterexamples can however be found in the literature: no core-hole effect is observed at the titanium or oxygen *K* edges in rutile TiO_2,[7,28] or at the oxygen *K* edge in NiO which are both semiconductors or insulators.[29] As a corollary of this assumption, it is widely believed that no core hole is needed to describe XANES or ELNES spectra related to pure metals because its screening by the valence electrons is efficient enough. Such an assumption is confirmed by studies of the lithium *K* edge in metallic systems such as pure lithium or $LiMn_2O_4$.[30] However, this argument does not hold from a fundamental point of view when considering self-consistent field (SCF) approaches since the screening cloud should, by definition of SCF, come out naturally. This paradox is illustrated by the fact that the core-hole effect was found to be important at the platinum metal $L_{2,3}$ and aluminum metal *K* edges.[31] A partial core hole was also needed to properly simulate the copper $L_{2,3}$ edges,[32] but the physics underlying such an *ad hoc* treatment remains unclear.

Another argument that can be found in the literature is that the core hole is better screened when the density of valence states is highly localized on the excited atom.[33] This argument was addressed to explain the weakness of the core-hole effect at the carbon *K* edge in transition-metal carbides.[34] However, several studies report that the core-hole effect is very strong at the oxygen *K* edge in MgO or Li_2O whereas the valence bands in these compounds mainly have an oxygen *p* character, or at the silicon *K* edge in pure silicon.[26,27,35–37] A last argument is given by De Groot *et al.*[38] The absence of a core-hole effect at the oxygen *K* edge for transition-metal oxides is justified by the fact that the first empty states being essentially localized on the transition-metal site, they are weakly affected by the core hole on the oxygen 1*s* orbital.

To include or not the core-hole effect into the calculation of ELNES or XANES spectra is thus a recurrent question for two reasons: the interpretations of experimental spectra can be severely impaired if this effect is not properly taken into account and its incorporation is not always an easy task to handle. In fact, for electronic structure codes based on the Bloch waves formalism, to include a core hole requires to build a supercell which drastically increases the number of atoms and thus the computation resources needed for the calculation.[39,40]

In short, no general rule can be deduced from all above cited examples, and the justifications for the core-hole strength at a given edge seem to vary from one system to another. The primary aim of this paper is to give a clear interpretation of the core-hole effect using DFT calculations and a general understanding of the underlying mechanisms governing its strength at a given edge. Let us emphasize that the present study is realized assuming the final-state rule, any discussion of the validity of which is beyond the scope of this paper. To do so, the WIEN2K (and its TELNES2 extension)[41] and FEFF (Ref. 17) codes were used to compute the ELNES (or XANES) spectra for various systems. Three model systems were studied: rutile TiO_2 (r-TiO_2), MgO, and pure 3*d* transition metals. The first two ones were selected since they were widely studied in the literature and, although being both oxides, they exhibit very different behavior with respect to the core-hole effect. We expect these two systems to be representative of the two extreme cases that can be encountered in such compounds. Concerning transition metals, they also exhibit a wide range of behavior allowing for a better understanding of the core-hole effect in metals. The response of the electronic structure to the creation of the core hole has been investigated under three aspects: the compensation charge mechanism occurring inside the solid due to the creation of the core hole, its impact on the excited atom projected local density of states (LDOS), and the influence of the core-hole depth on these modifications.

The paper is organized as follows. The first part deals with the computational methods. After that, results concerning the electronic structure modifications induced by the core hole are given. In the last part, the results are discussed: two rules are obtained concerning the localization and the symmetry of the levels perturbed by the core hole. These rules are illustrated by simulations related to the three above mentioned model systems.

II. COMPUTATIONAL METHODS

A. WIEN2K

WIEN2K calculations are based on a full-potential band-structure approach: valence or conduction KS wave functions are described as Bloch states. Wave functions (as well as potentials) are described in the whole space using a muffin-tin (MT) approach consisting of nonoverlapping spheres centered at each atomic site. No assumption is made

in the interstitial region about the shape of the potentials: WIEN2K is thus a full-potential code. Inside MT spheres, the KS wave functions are developed on a linearized augmented plane wave (LAPW) (Ref. 42) basis set or an augmented plane-wave (APW) basis set combined with local orbitals (APW+lo).[43] This second approach was used in the present paper. Plane waves are used in the interstitial space. The core states, needed for the calculation of the matrix elements of Eqs. (2) and (3), are calculated with a relativistic atomic code.[44,45] Calculations were performed within the generalized gradient approximation using the Perdew-Burke-Ernzerhof's potential for exchange and correlation.[46] ELNES and XANES calculations were performed using the TELNES2 extension of WIEN2K. All the parameters used for the calculations are given in Table VI (Appendix).

Two different approaches can be used to take the core hole into account in the SCF calculation: removing a given core electron of the excited atom or replacing the excited atom by its right neighbor in the periodic table (the so-called $Z+1$ approximation). In the present paper, the first approach was systematically used excepted for Zn where the $Z+1$ approximation has been considered. Due to periodic boundary conditions, 2^*2^*2 supercells were considered systematically in order to minimize mutual interactions between adjacent holes.[39] Although any residual interaction cannot be excluded, such a supercell size is typical of WIEN2K calculations including core holes: see Ref. 37 for MgO, Ref. 26 for Li_2O, and Refs. 34 and 54 concerning transition metals. Moreover, given the good agreement between WIEN2K and FEFF calculations, we are confident that adjacent holes interactions are of minor importance with respect to the effects in question.

B. FEFF

The FEFF code[17] (version 8.4) can be described as a real-space Korringa-Kohn-Rostoker[47,48] (KKR) approach. Being a Green's function method, it does not need to calculate the KS orbitals. Instead, FEFF uses as basis scattering states to represent the Green's function around each scattering center: it is therefore a real-space full multiple-scattering (RSFMS) method. One advantage of such a real-space approach is that FEFF allows linking the fine structures observed in an experimental spectrum to the geometry and to the chemical structure of the probed material which is not restricted to be periodic: nonperiodic systems can be studied alike. FEFF approximates the total electronic potential for the initial and final states with spherically averaged MT potentials centered on each atom. In this approximation, the potential is constant and flat in the interstitial region between the spheres: it is one of the main differences with WIEN2K that includes nonspherical corrections as noted above. However, nonspherical corrections to the potentials are roughly approximated by allowing the MT spheres to overlap (we always use the default value: overlap 15%). Furthermore, WIEN2K and FEFF differ in the treatment of the excited final states. In the former, a fully screened core hole and a GGA exchange-correlation potential are used, while in the later a central atom with a screened core hole and a GW self-energy $\Sigma(E)$ are considered. This last is analogous to the exchange-correlation potential used for the ground-state potential calculation. Even if it has been shown that it is possible to go beyond this approximation,[49] for all here presented results we have used the single plasmon-pole model of Hedin and Lundquist[50] implemented in FEFF for calculating this self-energy. To estimate the weight of the core-hole effect into calculated XANES or ELNES spectra, we have used the possibility offered by FEFF to switch off the core hole (NOHOLE card, see FEFF documentation).[51] It also exists other many-body effects that cause additional inelastic losses and affect the magnitude of the fine structures close to an edge onset.[52] They are traduced through an overall many-body amplitude reduction factor noted S_0^2 that depends weakly on the energy and that is generally kept constant.[2] We have use $S_0^2=0.9$, a value usually close to those accepted for pure metals. Being a cluster based method, FEFF needs to define the cluster size to be used to match the experimental data. The optimum parameters we have obtained using an s p d basis set are gathered in Table VII (Appendix). Furthermore, to compare with experimental spectra, all XANES spectra of pure metals have been convolved with a Gaussian [full width at half maximum (FWHM): 1 eV].

III. RESULTS

A. Charge compensation in the crystal

It is well documented that the $Z+1$ approximation and the explicit account of a core hole give rather similar results.[27] However, concerning the second method, one has to think about conserving the neutrality of the crystal (it is not ionized during a EELS or XAS experiment). In WIEN2K, the generally used approach is to introduce a background negative charge spread over the unit cell at the beginning of the calculation. It is then interesting to see how the overall charge density is reorganized due to the presence of the hole and of this background charge. We have thus investigated this reorganization for a core hole put either on an oxygen 1s or on a titanium $2p_{3/2}$ state in r-TiO_2 and for a 1s core hole created either on an oxygen or on a magnesium atom in MgO. Results obtained with WIEN2K are given in Table I for r-TiO_2 and MgO. In this table, the total and valence charges on the excited atom (labeled with a star) are compared to those calculated for the same atom in the ground-state (GS) configuration. The decomposition of the valence charge on the different angular quantum numbers is also given.

Focusing on the first two columns of Table I, one can see that either for the excited oxygen or the titanium one, the positive charge induced on the atom by the core hole is totally compensated at the end of the SCF loop. The background charge is entirely relocalized on the excited atom (see second column of Table I: the valence charge is systematically increased by one unit with respect to the ground-state configuration). Focusing on the decomposition of the valence charge on the different orbital symmetries, one observes that the extra charge is relocalized in a given atomic orbital of p symmetry concerning the oxygen atom and d symmetry for the titanium one. In short, in r-TiO_2 the charge compensation is made in the first empty atomic levels of the excited atom. From this point of view, the valence band of the excited atom

TABLE I. Projected total and valence charges inside the MTS obtained from WIEN2K for the oxygen or titanium atoms in r-TiO_2 (four first lines), and oxygen and magnesium in MgO (four last lines). In both cases, the excited (*) or ground-state ($_{GS}$) configurations are given for each atom. The decomposition of the valence charge on the different angular quantum numbers is also given. In brackets: difference between the excited and GS charges.

	Total charge	Valence charge	$l=0$ (s)	$l=1$ (p)	$l=2$ (d)
O^*	7.632 (+0.057)	6.632 (+1.057)	1.774 (+0.094)	4.832 (+0.96)	0.0181 (+0.0018)
O_{GS}	7.575	5.575	1.680	3.872	0.0163
Ti^*	19.275 (+0.021)	10.275 (+1.021)	2.072 (+0.013)	5.972 (+0.062)	2.243 (+1.003)
Ti_{GS}	19.254	9.254	2.059	5.910	1.240
O^*	8.115 (−0.148)	7.115 (+0.852)	1.880 (+0.086)	5.218 (+0.763)	0.0144 (+0.036)
O_{GS}	8.263	6.263	1.794	4.455	0.0108
Mg^*	9.719 (−0.653)	8.720 (+0.348)	2.269 (+0.135)	6.307 (+0.175)	0.122 (+0.035)
Mg_{GS}	10.372	8.372	2.134	6.132	0.087

is comparable to that of its next neighbor on the periodic table, a fact that justifies the equivalence with the $Z+1$ approximation. It should be mentioned that the valence charge of the first neighbor of the excited atom (not shown in Table I) is not modified by the presence of the core hole.

This compensating charge mechanism is very close to the one used in the FEFF code. In this approach, the extra charge is relocalized in the muffin-tin sphere (MTS) of the excited atom at the beginning of the calculation so that the electronic configuration obtained at the end of the SCF loop is very close to that found with WIEN2K. This can be seen in Table II where the results obtained with FEFF are collected: the extra charge is also mainly localized in the oxygen p LDOS for an oxygen $1s$ core hole and in the titanium d bands when considering a titanium 2 $p_{3/2}$ core hole. It should however be noticed that charge values can differ from one code to the other, especially for the titanium and magnesium atoms or the transition metals (see Tables III and IV). One can find two reasons for such discrepancies. First of all, the separations between valence and core states are hold differently in these two codes which explains that the charge values per orbital quantum number can differ significantly. For instance, the magnesium $3s$ and $3p$ states are treated as valence states in WIEN2K and as core states in FEFF so that 6.307 p states are found for the magnesium GS configuration in Table I and 0.709 in Table II. Differences can also be observed when comparing the calculated valence charge differences between the GS and the excited configurations obtained with WIEN2K or FEFF. For instance, the difference is larger for the magnesium p states in FEFF (+0.438) than in WIEN2K (+0.175). Similar discrepancies are observed when focusing on the p states of the end members of the transition-metal series (see copper and zinc in Tables III and IV). Such differences can be attributed to the different descriptions of the potentials. WIEN2K is based on a full-potential approach whereas FEFF use overlapped (15%) muffin-tin potentials. For delocalized states such as the magnesium or the transition metals p states, this can lead to significant differences since a nonnegligible part of the charge density is delocalized in the interstitial region. However, when considering localized states such as transition metals d states, the muffin-tin approximation comes to be a good approximation so that WIEN2K and FEFF results are in much better agreement (compare the last columns of Tables III and IV).

TABLE II. Decomposition of the valence charge in r-TiO_2 and MgO as in Table I obtained from FEFF. In brackets: difference between the excited and GS charges.

	$l=0$ (s)	$l=1$ (p)	$l=2$ (d)
O^*	1.876 (+0.036)	5.09 (+0.692)	0.054 (−0.012)
O_{GS}	1.84	4.398	0.066
Ti^*	0.404 (+0.007)	6.702 (+0.035)	3.490 (+1.154)
Ti_{GS}	0.397	6.667	2.336
O^*	1.87 (+0.049)	5.108 (+0.569)	0.013 (−0.002)
O_{GS}	1.821	4.539	0.015
Mg^*	0.800 (+0.359)	1.147 (+0.438)	0.640 (+0.166)
Mg_{GS}	0.441	0.709	0.474

To conclude this discussion, it is worth mentioning that the overlap of the muffin-tin spheres makes that FEFF double counts charge in the region where two MTS overlap and does not count charge at all in the region not covered by any sphere.[17] We have not tested how this overlap influences the charge distributions reported in Tables II and IV. It should be added that R_{SCF} (see Table VII) also impacts the results due to surface states of the cluster: in fact we have verified that to increase R_{SCF} beyond the values quoted in Table VII only affects the FEFF charge distributions marginally.

Coming back to the charge compensation mechanism, it can be seen that the situation in MgO is rather different from that in r-TiO_2. Focusing first on WIEN2K calculations (Table I), one can see that the background charge is not totally relocalized on the excited atom at the end of the SCF loop. The charge compensation is higher on the oxygen atom than on the magnesium one, but there is still a lack of 0.148 electron on O^*. The remaining charge is not delocalized on the neighboring atoms: it is located into the interstitial region. This delocalization goes with a repartition of the compensating charge on different atomic orbitals. This is particularly visible for the magnesium atom where the +0.348 electron is mainly shared between the s orbitals (0.135) and

TABLE III. Projected total and valence charges inside the MTS related to the excited (*) or ground state ($_{GS}$) configurations obtained from WIEN2K for some transition metals. For each atom, the decomposition of the valence charge on the different angular quantum numbers is also given. In brackets: difference between the excited and GS charges.

	Total charge	Valence charge	$l=0$ (s)	$l=1$ (p)	$l=2$ (d)
Ti^*	20.668 (+0.112)	11.668 (+1.112)	2.344 (+0.022)	6.267 (+0.042)	3.044 (+1.05)
Ti_{GS}	20.556	10.556	2.322	6.225	1.994
Fe^*	25.083 (+0.097)	14.084 (+1.096)	0.412 (+0.004)	6.411 (+0.006)	7.222 (+1.089)
Fe_{GS}	24.986	12.988	0.408	6.405	6.133
Co^*	26.130 (−0.048)	15.235 (+1.055)	0.459 (+0.005)	6.466 (+0.011)	8.265 (+1.04)
Co_{GS}	26.178	14.180	0.454	6.455	7.225
Cu^*	28.085 (−0.235)	17.085 (+0.766)	0.637 (+0.114)	6.607 (+0.137)	9.802 (+0.512)
Cu_{GS}	28.32	16.319	0.523	6.470	9.290
Zn^*	29.565 (+0.422)	11.566 (+0.422)	0.923 (+0.21)	0.692 (+0.099)	9.939 (+0.12)
Zn_{GS}	29.143	11.144	0.713	0.593	9.819

the p ones (+0.175). Such a difference for the charge compensation between r-TiO_2 and MgO can be understood when focusing on the projected DOS as well as on the localization of the electronic densities around the Fermi level. The LDOS for r-TiO_2 and MgO are plotted in Fig. 1, and two-dimensional (2D) projections of the electronic densities in the dense plane of both structures are presented in Fig. 2. Results presented in these two figures were obtained with WIEN2K.

Looking first at the valence bands, it can be observed that they have mainly an O p character in both materials. The charge densities corresponding to the last occupied levels represent thus, to a good approximation, the O p states in these two compounds. The main difference lies in the difference of spatial extension of these O p states: it is clear from the plotted densities that the O p charge density is much more contracted in r-TiO_2 than in MgO (see Fig. 2). This is not a question of bond distance since the Ti-O bond is smaller than the Mg-O one (1.946 and 2.108 Å, respectively). The extra charge relocalized in the O p band is thus more localized on the oxygen atom in r-TiO_2 than in MgO. Concerning the compensating charge on Mg or Ti, the difference is much more pronounced. Focusing on the conduction band in r-TiO_2, one can see that it has mainly a titanium d character (Fig. 1), the corresponding charge density being strongly localized on the titanium atom [Fig. 2(a)]. The extra charge relocalized in the d states of the excited titanium atom is thus strongly localized on it. On the opposite, the first states of the conduction band in MgO have oxygen and magnesium s and p characters (Fig. 1). The compensating charge on the excited Mg atom will thus be spread on the s and p states and highly delocalized into the interstitial region. The situation here observed is equivalent to the one reported in the literature concerning the charge compensation in transition-metal silicides.[53]

The charge compensation mechanism we observe for r-TiO_2 and MgO is very general and can be extended to other materials. For example, Tables III (results from WIEN2K) and IV (results from FEFF) show the charge compensation resulting from a $1s$ core hole for some transition metals when going from titanium to zinc. Considering first the results obtained with WIEN2K (Table III), one can see that the situation is very similar from titanium to cobalt: the extra charge goes into an empty d state. For copper and zinc, it is different since the d band is nearly filled in the GS (9.290 and 9.819 d electrons for copper and zinc, respectively). The extra charge

TABLE IV. Same quantities as in Table III obtained from FEFF.

	Total charge	Valence charge	$l=0$ (s)	$l=1$ (p)	$l=2$ (d)
Ti^*	22	11.18 (+1.18)	0.672 (+0.007)	6.856 (+0.0652)	3.652 (+1.111)
Ti_{GS}	22	10	0.665	6.794	2.541
Fe^*	26	9.037 (+1.037)	0.617 (−0.0004)	0.770 (+0.006)	7.65 (+1.035)
Fe_{GS}	26	8	0.621	0.764	6.615
Co^*	27	10 (+1.0)	0.623 (−0.002)	0.740 (+0.005)	8.638 (+0.998)
Co_{GS}	27	9	0.625	0.735	7.64
Cu^*	29	12.076 (+1.076)	0.911 (+0.218)	1.092 (+0.339)	10.073 (+0.519)
Cu_{GS}	29	11	0.693	0.753	9.554
Zn^*	30	13.164 (+1.164)	1.377 (+0.371)	1.544 (+0.58)	10.243 (+0.207)
Zn_{GS}	30	12	1.006	0.958	10.036

TABLE V. WIEN2K projected total and valence charges inside the MTS of the titanium atom in r-TiO_2 considering either a 1*s*, 2*s*, or $2p_{3/2}$ core hole and the GS configuration.

	Total charge	Valence charge	l=0 (*s*)	l=1 (*p*)	l=2 (*d*)
Ti^*_{1s}	19.275	10.275 (+1.021)	2.082 (+0.023)	6.003 (+0.093)	2.146 (+0.906)
Ti^*_{2s}	19.334	10.334 (+1.08)	2.071 (+0.012)	5.968 (+0.058)	2.251 (+1.011)
$Ti^*_{2p_{3/2}}$	19.331	10.332 (+1.078)	2.072 (+0.013)	5.972 (+0.062)	2.243 (+1.003)
Ti_{GS}	19.254	9.254	2.059	5.91	1.240

is thus spread over the remaining *d* states and the 4*s* and 4*p* orbitals. The *s* and *p* states being much more delocalized than the *d* ones, the compensating charge leaks out of the MTS and the valence charge compensation decreases. The evolution observed with FEFF is identical (see Table III): one observes a decreasing *d* character (and an increasing *s* and *p* one) of the compensating charge when going from titanium to zinc. An equivalent mechanism was proposed in transition metals when considering the core-hole screening effect in the initial state of Auger emission.[54]

B. Modifications on the excited atom projected LDOS

The localization of the wave function also governs the way the electronic structure is relaxed in the presence of a core hole on a given atom. This is very important for ELNES or XANES simulations since, for one-electron excitations, the fine structures observed experimentally are directly linked the unoccupied LDOS projected on the excited atom. Comparison between the oxygen *p* and titanium *d* LDOS calculated with WIEN2K considering or not a core hole in r-TiO_2 are shown in Fig. 3. FEFF calculations, not shown here, give very similar results. Focusing first on the oxygen DOS, it is obvious that the weight of the excited oxygen *p* LDOS is transferred at the bottom of the valence band (between −8.8 and −6.8 eV) where intense sharp peaks are observed. This is a clear signature of the localization of the extra electron in the oxygen *p* band. On the contrary, the empty states are weakly affected by the core hole: no extra peak is observed and the relative intensities of the two main peaks just above the Fermi level (between 2 and 8 eV) are very close to that of the ground-state calculation. The core-hole effect at the oxygen *K* edge is thus weak.[7,28,55] On the other hand, a core hole on the titanium atom has almost no effect on the occupied titanium *d* LDOS as illustrated by Fig. 3. The only impact of the extra *d* electron is the growth of a small peak located at the bottom of the valence band. The empty titanium *d* LDOS is however much more affected by the core hole: an intense localized peak appears just above the Fermi level. This can be viewed as the antibonding state corresponding the localized *d* electron. The core-hole effect at the titanium L_3 edge is thus expected to be very strong. The difference of core-hole effect between the oxygen *K* and the titanium L_3 edge in r-TiO_2 observed by Heiliger *et al.* is thus a direct consequence of the existence or not of such modifications on the oxygen *p* and titanium *d* LDOS.[55]

The same study can be performed on the oxygen and magnesium *p* LDOS in MgO: results obtained with or with-

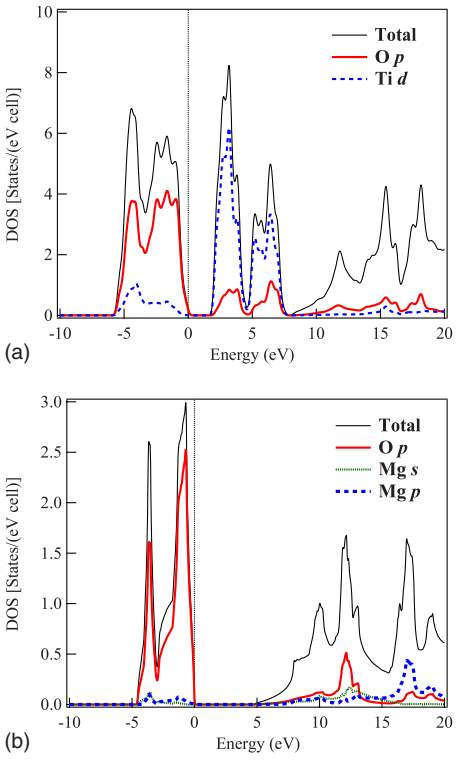

FIG. 1. (Color online) Total and projected DOS for r-TiO_2 (top) and MgO (bottom) obtained with WIEN2K.

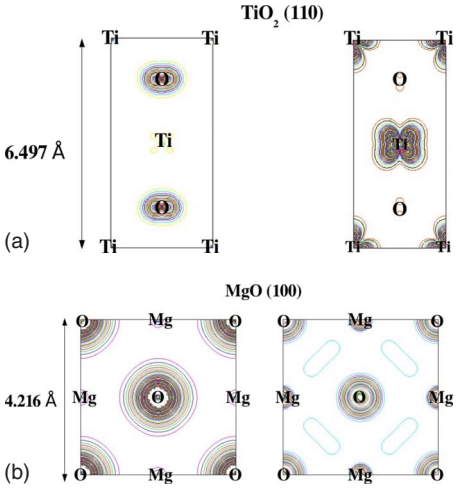

FIG. 2. (Color online) Electronic densities corresponding to the last occupied (left) and first unoccupied (right) bands projected in a (110) plane of TiO_2 (a) and (100) plane of MgO (b). The same values were used to plot the isolines.

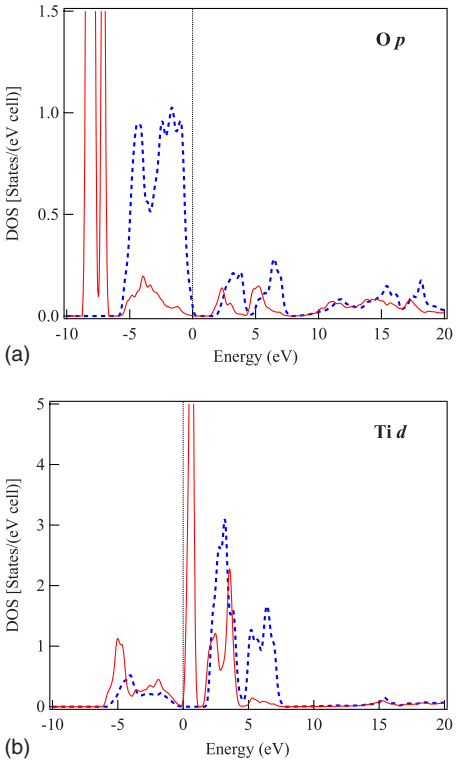

FIG. 3. (Color online) Oxygen p LDOS (top) in r-TiO_2 with (full lines) or without (dotted lines) a 1s core hole on the oxygen atom. Titanium d LDOS (bottom) in r-TiO_2 with (full lines) or without (dotted lines) a $2p_{3/2}$ core hole on the titanium atom.

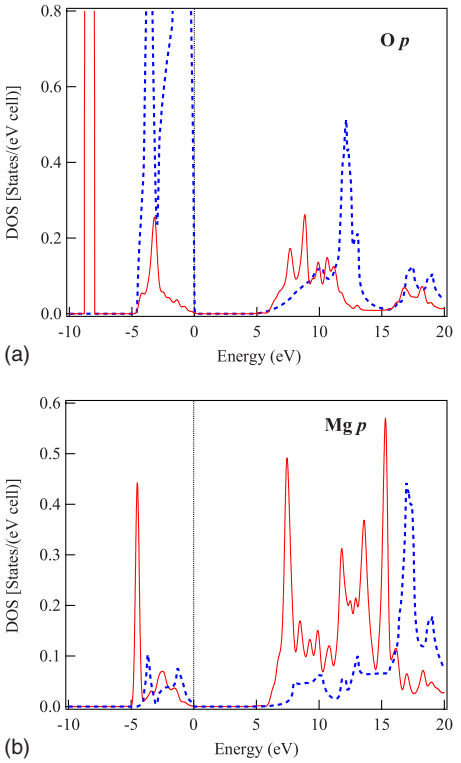

FIG. 4. (Color online) Oxygen (top) and magnesium (bottom) p LDOS in MgO with (full lines) or without (dotted lines) a 1s core hole.

out a 1s core hole on each atom are presented in Fig. 4. The core-hole effect on the O p LDOS in the valence band (VB) is similar to the one observed for r-TiO_2. A strong localized peak appears below the VB (around −8.4 eV) and the weight of the excited oxygen atom in this band is strongly reduced. However, contrary to r-TiO_2, the O p LDOS in the conduction band (CB) is also strongly modified. The intense peak located at 12.5 eV in the GS LDOS has disappeared and several new structures appear below 10 eV. As already reported in several studies, the core hole must be explicitly taken into account to get simulations of the O K edge in good agreement with the experiments.[27,35] The situation is similar for the magnesium p LDOS. A new structure is created at the bottom of the VB; however, it is less intense than the one observed in the O p LDOS and it is not clearly separated from the VB. This suggests that the core-hole effect is less intense on the magnesium states in the VB than on the oxygen ones. Considering now the CB, strong modifications are induced by the core hole: the intense peak around 18 eV has disappeared and several important structures appear below 15 eV. As mentioned in several papers, the core-hole effect at the magnesium K edge is important.[27,37,35] The core-hole effects in r-TiO_2 and MgO are thus different: if both metallic sites are affected by the presence of a core hole, this is not the case for the oxygen atom. The oxygen unoccupied p LDOS is not affected in r-TiO_2 whereas a clear effect is observed in MgO.

The impact of a core hole on a given wave function in the solid is strongly related to the spatial localization (Fig. 2) and to the weight of the atom that will be excited (e.g., which contains the core hole) in the considered wave function. Indeed, the importance of the core-hole effect can be discussed qualitatively considering the perturbation ΔE induced by the creation of a core hole on the eigenenergies of the system in its ground state. This can be achieved by considering the standard stationary perturbation theory applied to a given valence or conduction wave function,[56] the perturbation $\hat{W}$ being mainly related to the difference of the atomic potentials felt by the electrons in the ground and excited states. This approach is well suited to Bloch states as obtained in WIEN2K since they are stationary solutions of the time-independent Schrödinger equation for the solid.[57] For simplicity, let us consider a binary system AB in its GS with one atomic orbital $|\phi_A\rangle$ and $|\phi_B\rangle$ per atomic site. In that case, an eigenvector $|\Psi\rangle$ of eigenvalue E_0 of the AB system can be written as

$$|\Psi\rangle = C_A \cdot |\phi_A\rangle + C_B \cdot |\phi_B\rangle. \tag{4}$$

Assuming that the overlap integral $\langle\phi_A|\phi_B\rangle$ is negligible (e.g., $|\phi_A\rangle$ and $|\phi_B\rangle$ is a basis set), the normalization of $|\Psi\rangle$ imposes that

$$|C_A|^2 + |C_B|^2 = 1. \tag{5}$$

Let us now consider the effect of the perturbation $\hat{W}$ induced by the removal of a core electron from atom A on the eigenvalue E_0. To the first order, the total perturbation on this eigenvalue is given by

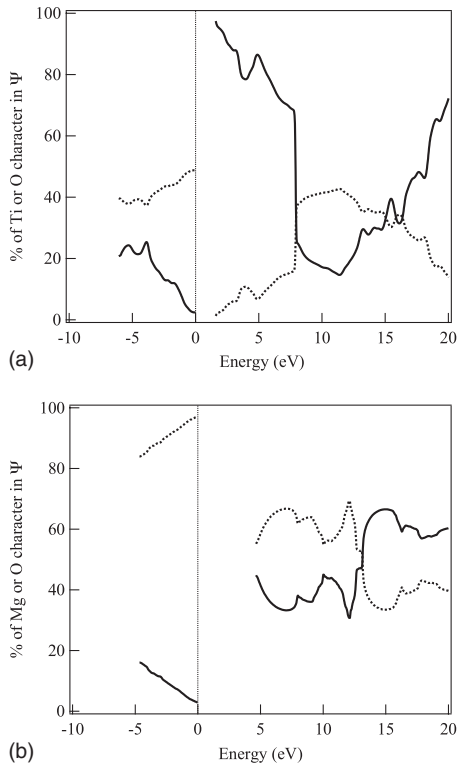

FIG. 5. Percentage of oxygen (dotted line) and titanium or magnesium (full line) character in the wave function for r-TiO_2 (top) and MgO (bottom).

$$\Delta E = E_n - E_0 = \langle \Psi | \hat{W} | \Psi \rangle. \tag{6}$$

ΔE can thus be expressed as a sum of three terms,

$$\Delta E = |C_A|^2 \langle \phi_A | \hat{W} | \phi_A \rangle + |C_B|^2 \langle \phi_B | \hat{W} | \phi_B \rangle + 2\,\mathrm{Re}(C_A^* \cdot C_B \langle \phi_A | \hat{W} | \phi_B \rangle). \tag{7}$$

It remains to know the values of the coefficients entering in Eqs. (4)–(7). The coefficients $|C_{A,B}|^2$ can be estimated from the DOS as follows. For each compound here studied, we divide the sum of the projected LDOS for a given atom (Ti, Mg, or O) by the total DOS, restricting these summations to the MTS, e.g., we neglect the contribution of the interstitial region. The results obtained within this framework are plotted in Fig. 5. Here again, for sake of simplicity, only the results obtained from WIEN2K calculations are reported, but FEFF calculations give very similar results. The multiplicity of the atoms in the unit cell was taken into account for these calculations; it explains that the oxygen weight in r-TiO_2 cannot exceed 50%. It can be seen from Fig. 5 that the VB in r-TiO_2 has predominantly an O character (like in MgO) whereas the first conduction states have a marked titanium character. In MgO, Mg and O atoms have nearly equal weight in the CB: this is the main difference between these two materials.

Let us apply Eq. (7) to a conduction state in r-TiO_2 just above the gap, considering that atom A is a titanium atom and B is an oxygen one. In this case, $C_{\mathrm{Ti}} \gg C_{\mathrm{O}}$ from Fig. 5. If the perturbation (e.g., the core hole) is localized on the titanium atom, all matrix elements involving $\hat{W}$ and the atomic orbital $|\phi_{\mathrm{O}}\rangle$ can be neglected because of the strong localization of $\hat{W}$ on the titanium. Only the first matrix element in Eq. (7) remains non-negligible. The coefficient C_{Ti} being much higher than C_{O}, the perturbation on $|\Psi\rangle$ is then important. Considering now the core hole on an oxygen atom, the only significant matrix element in ΔE is the second one in Eq. (7). However, the prefactor $|C_{\mathrm{O}}|^2$ is then very small compared to unity (see Fig. 5) so that the global perturbation ΔE is also small: $|\Psi\rangle$ is then weakly affected by the perturbation. This just is what is observed on the LDOS including the core hole reported in Fig. 3. In the first case, the core hole being localized on the titanium atom (Fig. 3 bottom), the first conduction states are strongly affected by the core hole and so is the titanium d LDOS. On the contrary, when the core hole is localized on the oxygen atom, the first conduction states are weakly affected so that the O p LDOS in the corresponding energy range is fairly insensitive to the core hole (Fig. 3 top). The situation is reversed when considering states in the VB: C_{O} is then much higher than C_{Ti} and the effect of the perturbation on valence states is much more important when the core hole is located on an oxygen atom than on a titanium one.

This line of reasoning is transposable to MgO. Let us consider a state $|\Psi\rangle$ corresponding to a conduction state for which $|C_{\mathrm{O}}|^2 \approx |C_{\mathrm{Mg}}|^2$ (Fig. 5). In such a case, whatever the localization of the core hole is, the matrix elements $\langle \phi_{\mathrm{O}} | \hat{W} | \phi_{\mathrm{O}} \rangle$ or $\langle \phi_{\mathrm{Mg}} | \hat{W} | \phi_{\mathrm{Mg}} \rangle$ are associated to a non-negligible prefactor $|C_{\mathrm{O}}|^2$ or $|C_{\mathrm{Mg}}|^2$. Thus, ΔE is significant in both cases: $|\Psi\rangle$ is then modified in any case and a core-hole effect is observed at both O K and Mg K edges. Considering Eq. (7), it is also obvious that the localization of the wave functions is a crucial parameter when evaluating the different matrix elements between the perturbation $\hat{W}$ and the different atomic orbitals.

Even if such a model is oversimplified, nevertheless it emphasizes two important factors to consider when analyzing the importance of the core-hole effect on an EELS or XAS experimental spectrum: the weight of the wave function on the different atomic sites of the crystal and the localization of the wave functions.

C. Influence of the core-hole depth

In this section, we address a third important criterion: the influence of the core-hole depth, i.e., the energy of the excited core level, on the perturbation. To do so, we compare the effect induced in r-TiO_2 by a titanium 1s or 2s core hole to that obtained with a $2p_{3/2}$ one as considered before. Results obtained in terms of charge compensation are given in Table V. Comparing the values obtained with these three core holes, the observed compensation mechanism is very similar: the valence charge is always increased by one electron. However when focusing on the distribution of this charge on the different angular momenta, the 1s core hole differs slightly from the two others: the charge is not entirely relocalized in the empty d states, but it is spread for 90% in the d states and for 10% in states of s and p symmetries. The

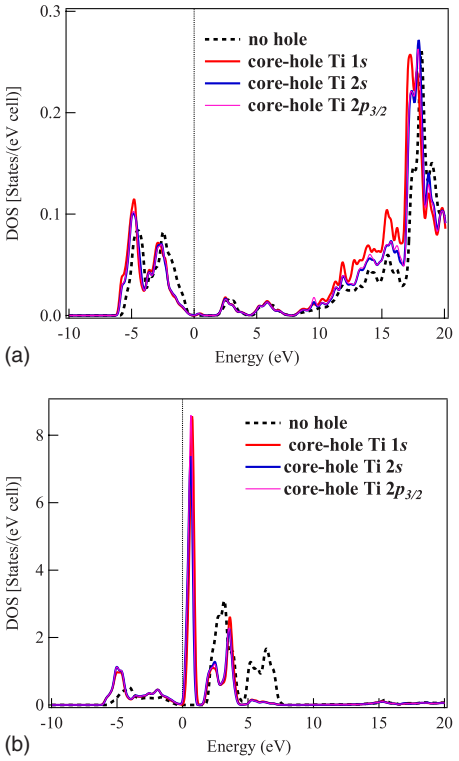

FIG. 6. (Color online) Comparison of the projected titanium $(s+p)$ (top) or titanium d (bottom) LDOS in r-TiO_2 when considering the ground state or different core holes.

same value of 0.9 extra d electron was found when using a full-potential multiple-scattering approach.[58] This is however a weak difference and the comparison of the $(s+p)$ and d LDOS plotted in Fig. 6 shows that whatever the core-hole depth is, its impact on the LDOS is rather similar. The titanium $(s+p)$ LDOS is not affected by the core hole and is found to be identical to that of a ground-state calculation in all cases. Concerning the titanium d DOS, whatever the core-hole depth is, the previously mentioned strong modifications are observed: the strong extra peak above the Fermi level appears in the three cases. Figure 6 illustrates an important point: only the bands where the extra charge is relocalized are affected by the core hole.

To have a more quantitative evaluation of the core-hole depth impact, one can have a look at the evolution of the screening properties of r-TiO_2 when considering the three kinds of core holes. Within the linear-response theory, the screening properties of a material, with respect to an external electromagnetic field, are given by the square modulus of the complex dielectric function: $\epsilon(\mathbf{q},\omega)\cdot\epsilon^*(\mathbf{q},\omega)$.[59] The complex dielectric function of r-TiO_2 in its ground state and considering the three different core holes was calculated using the OPTIC extension of WIEN2K (calculations are performed for $\mathbf{q}=0$).[60] DFT calculations were already proven to give a good description of the dielectric response of r-TiO_2 (at least concerning the static dielectric constant).[61] For the calculations including the core holes, 2^*2^*2 supercells were used. Results are presented in Fig. 7 for the first ten eV.

Above two eV, the main change in the screening function is the decrease in the intensity of the two strong peaks lo-

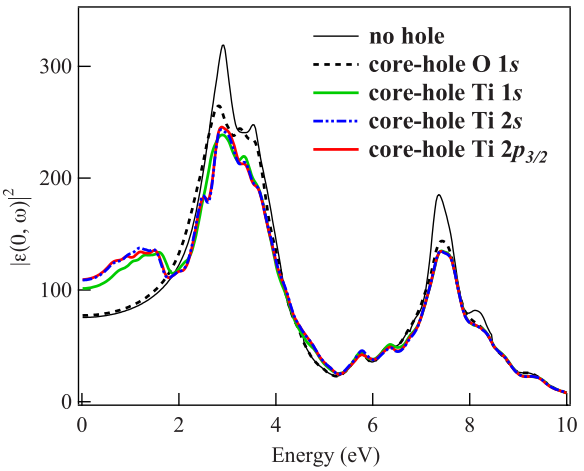

FIG. 7. (Color online) Square modulus of the complex dielectric function of r-TiO_2 calculated (WIEN2K) for the ground state and for some excited configurations.

cated around 3 and 7.5 eV. Whatever the localization of the core hole is, the screening functions are very similar in this energy range. Below 2 eV, significant changes can be observed: the localization of the core hole has an impact in this energy range. With a core hole on the oxygen atom, the screening function is equivalent to that of the ground-state calculation. This can be linked to the fact that the core-hole effect principally modifies the electronic structure below the VB and not around the Fermi level. When localizing it on a titanium atom, the screening is clearly increased. This can be related to the appearance of the strong localized peak observed just above the Fermi level in the titanium d LDOS in Fig. 6. If the screening functions calculated with a $2s$ or $2p_{3/2}$ core hole have similar intensities, it is slightly decreased when the core hole is localized on the titanium $1s$ orbital. As stated a long time ago by Slater,[62] a $1s$ core hole is intrinsically more screened by the remaining electrons of the atom than a core hole created in more external orbitals where a part of the core electrons becomes less efficient for its screening. As a consequence, the compensating charge on the excited atom is less localized and a small part is transferred from the d to s and p orbitals as observed in Table V. The resulting screening is slightly reduced. When considering deep core levels, the core-hole depth has thus an impact on the screening properties of the material but as far as the LDOS are concerned, the variations are very small. The core-hole effect on ELNES or XANES spectra should then be very similar. The situation can be different when considering less tightly bound levels: Nufer *et al.* have shown for instance that the the core-hole effect is very different when considering either the aluminum K or L_1 edges in α-Al_2O_3.[63]

IV. DISCUSSION

Results presented here evidence that the perturbation due to a core hole on a deep core level is localized on the excited atom. The compensating charge, necessary to maintain the neutrality of the crystal (fully relaxed configuration), is more or less entirely relocalized on the excited atom depending on

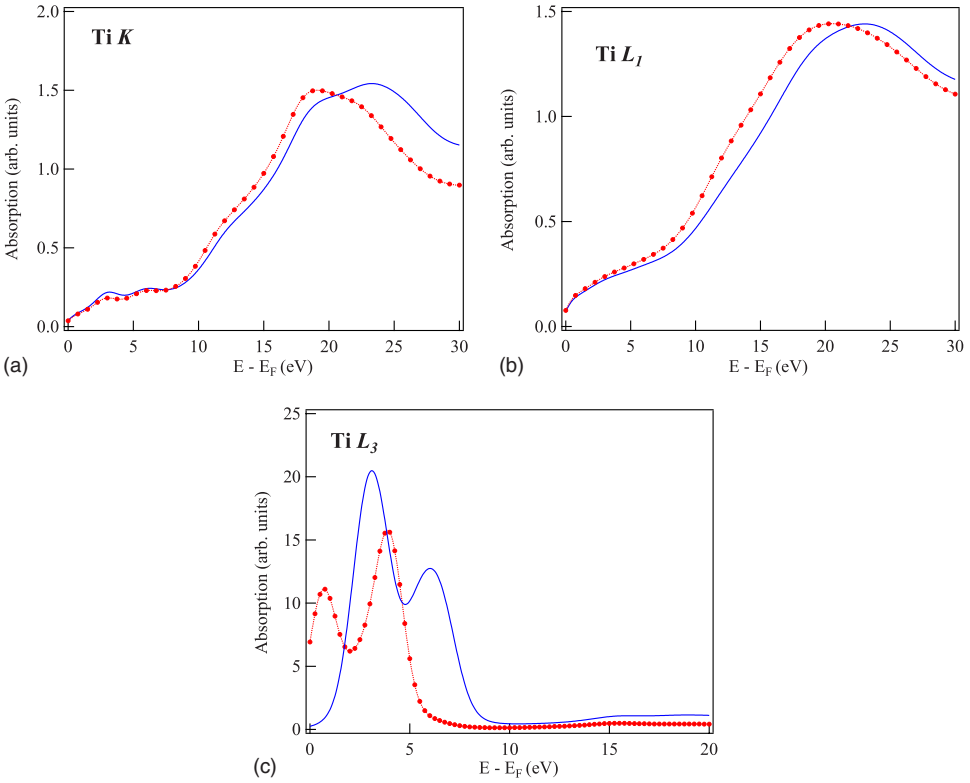

FIG. 8. (Color online) Comparison of the Ti K, Ti L_1, and Ti L_3 edges in r-TiO_2 calculated (WIEN2K) with (dotted line with circles) or without (full line) a core hole.

the localization of the corresponding wave function. Considering such an atomic process, the nature of the compensating charge can be roughly predicted as corresponding to the first empty atomic levels of the excited atom: mainly p character for an oxygen atom, s and p characters for a magnesium atom, d character for the early transition metals with increasing s and p contributions when going toward the end members of the series. When considering ELNES or XANES simulations, two criteria are found to be important: the weight of the excited atom in the first states above the Fermi level and the symmetry of the compensating charge.

The first point is of primary interest since it results that the impact of the core-hole effect is not linked to the metallic or insulating nature of the probed sample. The pertinent approach is to focus on the chemical nature of the first empty states. Considering this argument, it is clear that a core-hole effect is expected in all pure compounds, including metals, what justifies the core-hole effect observed at the platinum metal and copper $L_{2,3}$ edges or at the aluminum metal K edge.

When focusing on complex compounds, this argument allows understanding on which atomic site the core-hole effect will be important. For instance, considering transition-metal oxides, no core-hole effect is expected (and observed) at the oxygen K edge.[7,28,29] However, a strong core-hole effect is observed at the oxygen K edge in Li_2O.[26] This is not surprising when looking at the lithium oxide density of states (see Ref. 26): the bottom of the conduction band has clearly a strong oxygen p character. Focusing on $SrTiO_3$, the LDOS calculations of Orhan *et al.* show that the bottom of the conduction band has mainly titanium character, with no strontium and a small oxygen contribution.[64] This explains the absence of a core-hole effect observed at the Sr L_3 edge, the weak effect at the O K edge while a strong effect is observed when considering the titanium L_3 edge.[40]

The second crucial point is the nature of the compensating charge since it governs which symmetry of the wave function is perturbed by the presence of a core hole. This is illustrated in Figs. 8 and 9 where the titanium K, L_1, and L_3 edges in r-TiO_2 calculated with WIEN2K and FEFF are plotted. It is clear from these results that the core-hole effect is much more important on the titanium L_3 edge than on the two others. The L_3 white line is shifted by 3 eV in the WIEN2K simulation and the relative intensities of the two fine structures at the top of the edge are inverted whereas no effect can be observed on the titanium Ti L_1 edge excepted a small shift of the spectral weight in the WIEN2K simulation (no effect at all is observed in the FEFF calculation). The titanium K edge is a bit more sensitive to the core hole than the Ti L_1 edge, but the changes remain quite small, especially when focusing on the FEFF calculation. It is a general observation that the core-hole effect is always more pronounced in the WIEN2K calculations than in the FEFF ones. This might be due to the different formalisms considered in the two codes: a full-potential approach is used in WIEN2K whereas FEFF calculations are performed in the muffin-tin approximation.

The important core-hole effect observed at the Ti L_3 edge is correlated with the localization of the compensating charge in the titanium d sates for a $2p_{3/2}$ core hole (see Table V): the perturbation on these bands is then important and observed

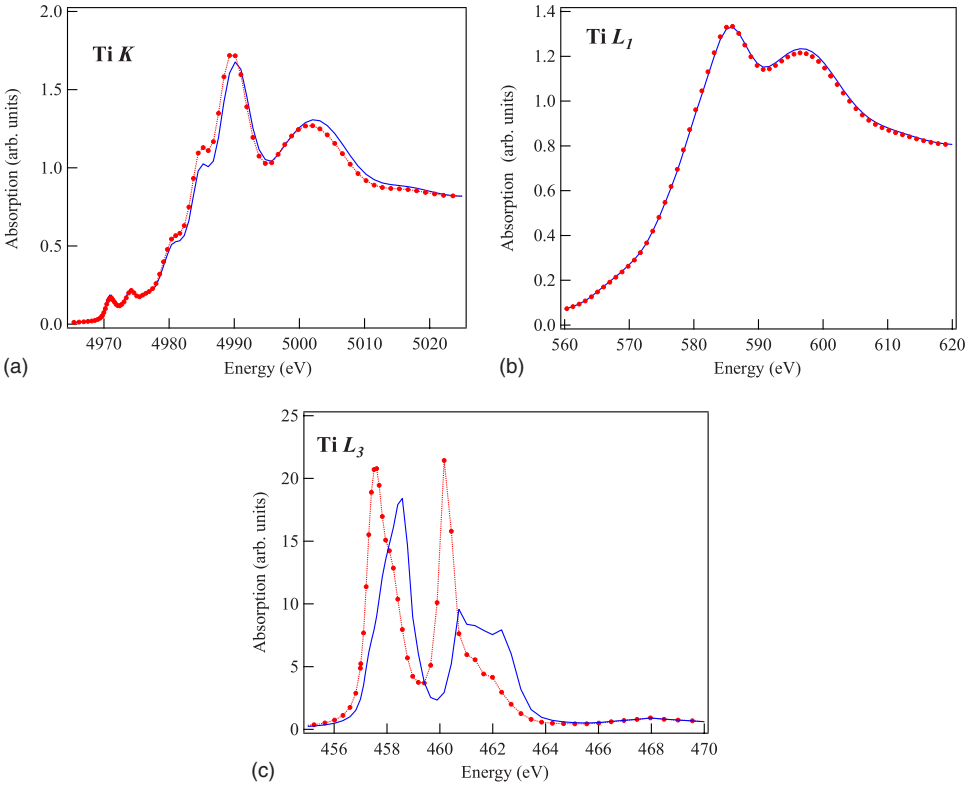

FIG. 9. (Color online) Comparison of the Ti K, Ti L_1, and Ti L_3 edges in r-TiO_2 calculated (FEFF) with (dotted line with circles) or without (full line) a core hole.

when probing the corresponding edge. Considering the Ti L_1 edge, the compensating charge being also localized in the titanium d bands, no effect is observed when probing the empty p density of states and therefore the core-hole effect is invisible at this edge. The dipole selection rule plays an important role here by imposing the symmetry of the unoccupied probed states. Finally the fact that the Ti K edge is more sensitive to the core-hole effect than the Ti L_1 one can be explained by the small part of the compensating charge introduced in the Ti (s,p) LDOS when a $1s$ core hole is created (see Table V).

Following the same line of reasoning and considering now Tables III and IV, one is able to predict a weak/inexistent core-hole effect at the K edges of the early transition metals and a more pronounced one when going to copper and zinc. Such predictions are confirmed by the examination of Figs. 10 and 11 where the results of calculations obtained with WIEN2K and FEFF are presented. It is clear from Fig. 11 that the core-hole effect for the first three metals is completely negligible and that it must be included in the two last cases to match the experimental spectra. Concerning the WIEN2K simulations, conclusions are identical. However, one can note a small decrease of the first peak's intensity at the titanium K edge when considering a core hole. Such a difference remains of minor importance when compared to experiment and would be reduced by increasing the broadening applied to the simulated spectra. This importance of the d band filling has already been mentioned by Tamura *et al.* to explain the observed core-hole effect at the platinum $L_{2,3}$ and aluminum K edges,[31] and by Yuan concerning the core-hole effect observed by Auger spectroscopy for transition metals.[54] The core-hole effect is thus mainly driven by the modification of the population of a given band. This is the reason why a strong core-hole effect is observed at the early transition metals $L_{2,3}$ edges where the compensating charge is fully relocalized in the d bands and both observed at the $L_{2,3}$ and K edges for copper and zinc where the compensating charge is spread over the s, p, and d states.

It can thus be concluded from these arguments that if a core hole is always present in a spectroscopic experiment, its effect is not always observed because it depends on the probed states. Two important criteria have been emphasized (1) the spatial localization of the first empty states, (2) the nature of the compensating charge. From these two criteria, two general rules can be given to explain the presence or not of a strong core-hole effect at a given edge when comparing experiments to calculations:

(1) for complex compounds, the core-hole effect is expected to be prominent for the atom that participates in the majority to the first empty states (this is the case of a titanium atom in r-TiO_2), and less sensitive on the other ones (the oxygen in r-TiO_2). When different atoms have an important weight, the core-hole effect is expected to be important on all of them (see the example of MgO). For pure materials, the core-hole effect is always present.

(2) For a given atom, only the LDOS having the same character as the compensating charge will be affected by the core hole. This compensating charge can be predicted to fill the first empty *atomic levels* of the excited atom.

These simple rules allow roughly predicting the core-hole effect strength at a given edge from the calculation point of

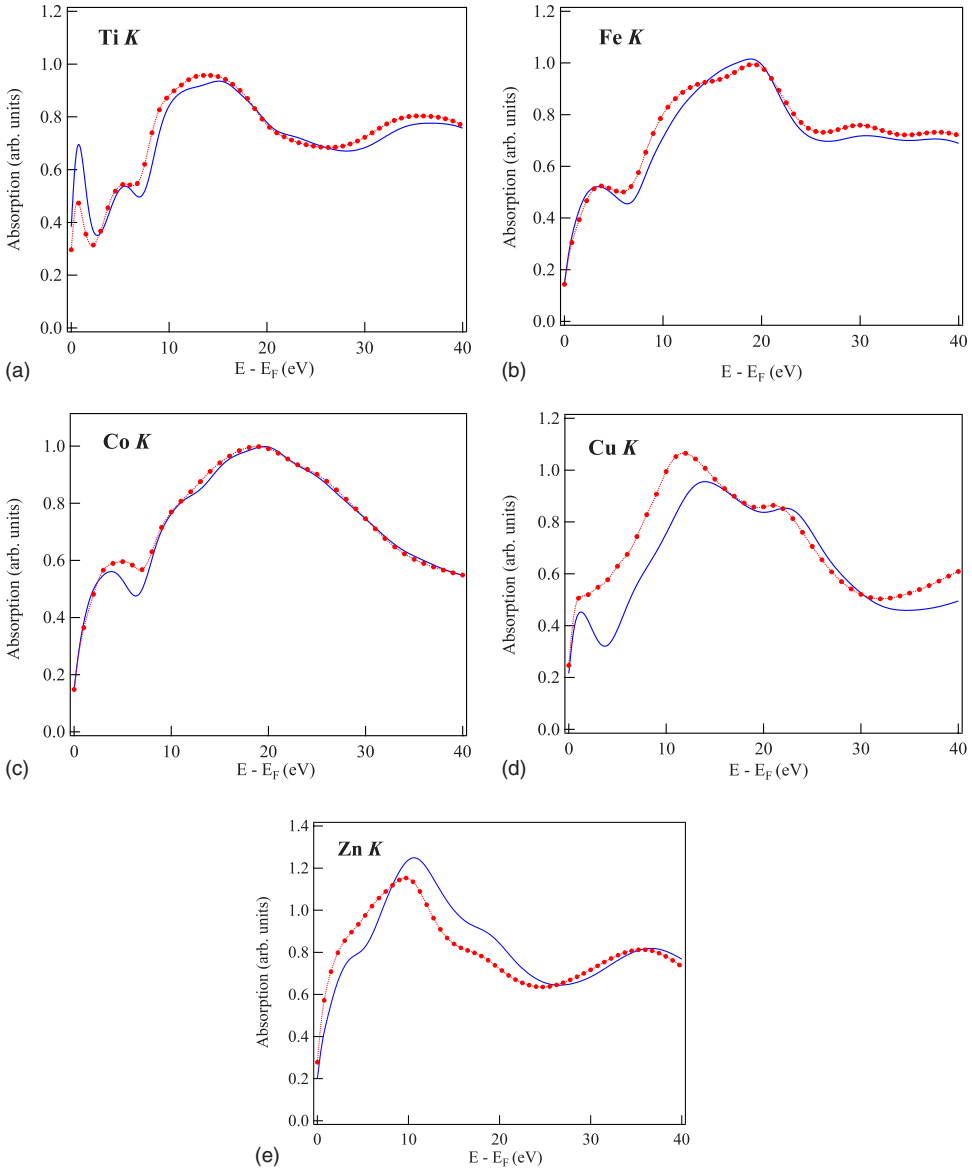

FIG. 10. (Color online) Calculated (WIEN2K) *K* edges for Ti, Fe, Co, Cu, and Zn with (dotted line with circles) or without (full line) a core hole.

view. In the cases for which the DFT formalism is known to be a good approximation (e.g., when the one-particle approximation is verified), this should give the justification for considering or not a core hole into the simulation. This is more satisfactory than the approach that consists in performing two simulations and keeping the one that best fits with the experiment. However, when considering edges where the DFT is not the optimal formalism, these rules just predict the effect of a core hole on the calculated edge, but nothing can be said *a priori* concerning the agreement or not with the experiment. It is well known that the core-hole effect is important in DFT calculations of the transition metal $L_{2,3}$ edges but generally ground-state calculations give better results when compared to experiment.[65] In this situation, the screening of the core hole is not well treated by the DFT and one should consider more complex approaches to obtain better agreement with the experiment.[66] Another example is the lithium *K* edge in pure metallic lithium. Here again a strong core-hole effect is predicted from the calculation as it can be observed in Fig. 12, but the ground-state calculation is in much better agreement with the experiment. Here again the validity of the DFT is questionable since the lithium 1*s* orbital is a semicore state and electron-hole interactions within delocalized wave functions should be treated with more complex formalisms.[67]

Finally, let us remark that the present analysis is different from the one recently proposed by Gao *et al.*[33] who study the core-hole effect in 1*s* core-level spectroscopy of the first-row elements. Compared with the experimental data, these authors show that one must use in the calculations a fully relaxed configuration (a core hole and an extra screening electron) to match the experimental spectra related to these light elements. Indeed, it is observed that the fine structures at the edge onset are repulsed toward higher energies when using an unrelaxed configuration (no core hole). Gao *et al.* deduce from an analysis of their results a relationship between the

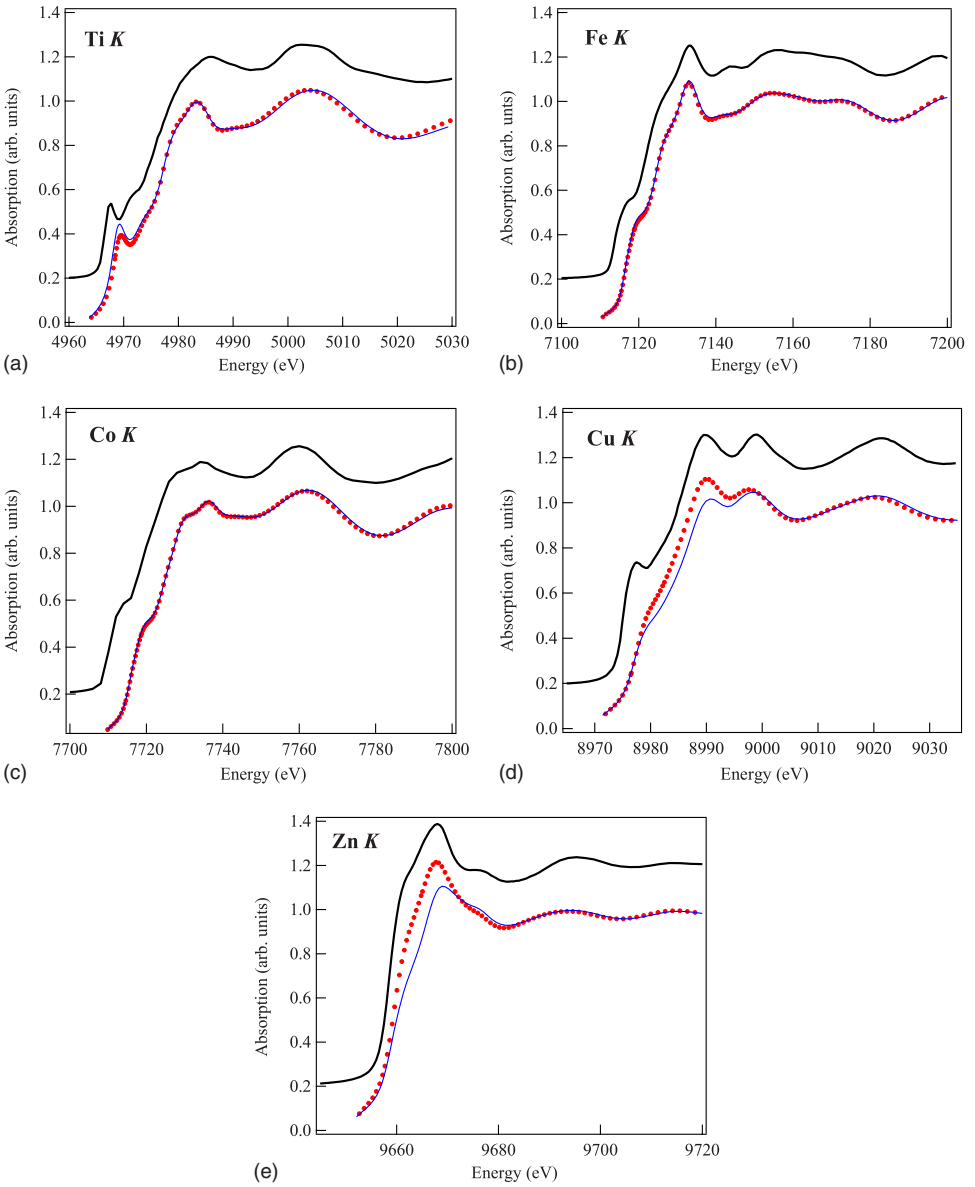

FIG. 11. (Color online) Calculated (FEFF) *K* edges for Ti, Fe, Co, Cu, and Zn with (circles) and without (full line) a core hole. Experimental spectra taken from the XANES database (thick black line) are also plotted for comparison.

VB charge population and the core-hole strength: larger differences between spectra seem to occur for smaller VB charge populations. However, as these authors note, the screening effect of valence electron populations is only an approximate index to rank the strength of the core hole. Indeed, it seems to be incompatible with what we found at the *K* edges of pure Cu and Zn (Figs. 10 and 11). In both cases, the core hole must be included to match the experimental data while it has a negligible effect for Ti, Fe, and Co (Figs. 10 and 11). This is in contradiction with the results of Gao *et al.* since the VB populations of the latter are smaller than those of the former that are nearly filled.

V. CONCLUSION

The electronic structure relaxation mechanism induced by a core hole has been investigated within the one-particle ap-

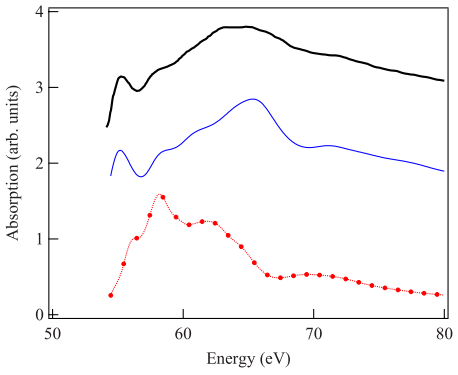

FIG. 12. (Color online) Li *K* edge calculated (WIEN2K) with (bottom) or without (middle) a core hole (Ref. 30). The experimental EELS spectrum (top) is taken from Ref. 30.

proximation using the density functional theory. Electronic structure calculations as well as ELNES/XANES simulations have been performed with two widely used codes: WIEN2K and FEFF.

Electronic structure calculations show that whatever edge is considered, the compensating charge introduced into the calculation to keep the crystal neutrality is systematically relocalized in the first empty states of the excited atom. In a highly ionic compound such as TiO_2, these states correspond to the first unoccupied levels of the *atomic* configuration for an isolated atom. The localization of these first empty states directly governs the spatial delocalization of this extracharge. In complex compounds, the nature of these first empty states governs the importance of the core-hole effect: if strongly localized on a given atom, it can be inferred from the here presented results that the core-hole effect will be prominent on this atom and rather small on the other ones. If equally spread over several atoms of the structure, the core-hole effect should be important on all these atoms. Another crucial parameter is the nature of this compensating charge which imposes, in a first approximation, which band will be most affected in the crystal and thus rules which edge will be affected by the core hole: it explains why a core-hole effect is observed at the titanium L_3 edge in r-TiO_2 and not at the K or L_1 ones. These results clearly show that a core-hole effect is always present in any core-level spectroscopy experiment but not always evidenced. Its importance is not driven by the metallic or insulating nature of the material, as sometimes mentioned, and only indirectly influenced by the density of valence electrons that would screen it. Our calculations however demonstrate the observation given by De Groot *et al.*[38] for transition-metal oxides: the core-hole effect at the oxygen K edge in transition-metal oxides is weak because the first empty states in the conduction band have a strong weight on the transition metal.

The influence of the core-hole depth on titanium in r-TiO_2 was also investigated and was shown to be negligible as far as the titanium LDOS is concerned. A more quantitative approach based on the calculation of the screening function shows however that a $1s$ core hole is more screened than outer shells electrons. Finally, compared to FEFF, it is observed that a full-potential approach such as the one implemented in WIEN2K is generally more sensitive to differences between GS and excited configurations when the core-hole effect strength is weak.

The presented results give a good description of what should the core-hole effect be like when considering edges that can be well described within the one-particle approximation. When the DFT is not the optimal formalism for describing the edge of interest, such results only explain the importance of the core-hole effect in the calculation but nothing can be said concerning the agreement with the experiment. The $L_{2,3}$ edges of transition metals or the lithium K edge in metallic lithium are good examples where a core-hole effect is expected, and observed, from DFT calculations. Nevertheless the agreement with the experiment is improved when considering a ground-state calculation, a result clearly emphasizing the limits of DFT.

ACKNOWLEDGMENTS

One of the authors (P.S.) thanks the University of Poitiers for hospitality, where part of this work was carried out. Part of the WIEN2K calculations presented in this work were performed at the "Centre régional de Calcul Intensif des Pays de la Loire" financed by the French Research Ministry, the "Région Pays de la Loire" and the University of Nantes.

APPENDIX

TABLE VI. Main parameters used for the WIEN2K calculations. The numbers in the SCF k-point columns refer to the sampling of the full Brillouin zone. Muffin-tin radii (R_{MT}) are given in bohr and K_{max} defines the wave-vector cutoff for the plane waves in the interstitial space.

	R_{MT}	$R_{MT}K_{max}$	k points (SCF)	k points (ELNES)
	Mg: 1.98		7*7*7	
MgO	O: 1.98	8.0	Supercell: 3*3*3	
	Ti: 1.94		8*8*13	6*6*9
TiO_2	O: 1.72	7.0	Supercell: 6*6*4	Supercell: 4*4*6
			24*24*13	8*8*4
Ti	2.00	8.0	Supercell: 12*12*6	Supercell: 4*4*2
			22*22*22	8*8*8
Fe	2.33	7.50	Supercell: 11*11*11	Supercell: 4*4*4
			28*28*15	9*9*5
Co	2.34	7.50	Supercell: 14*14*7	Supercell: 4*4*2
			18*18*18	6*6*6
Cu	2.40	7.50	Supercell: 9*9*9	Supercell: 3*3*3
			25*25*12	8*8*4
Zn	2.50	7.50	Supercell: 13*13*5	Supercell: 4*4*2
			17*17*17	9*9*9
Li	2.85	7.0	Supercell: 8*8*8	Supercell: 4*4*4

TABLE VII. Main parameters used for the FEFF calculations. R_{SCF} refers to the size of the clusters used to obtain reliable potentials from the SCF loop while R_{FMS} is the size of the clusters (including N_{atoms}) used for calculating the XANES spectra.

	Edge	R_{SCF} (Å)	R_{FMS} (Å)	N_{atoms}
Pure Metals	Ti K	4	7	81
	Fe K	4.1	6	65
	Co K	4	6	81
	Ni K	4	6.2	87
	Cu K	4	8	177
	Zn K	4	8	135
TiO_2	Ti K	4.6	7.9	197
	O K	4.6	7.9	197
	Ti L_3	4.6	7	137
	Ti L_1	4.6	7	137
MgO	Mg K	4	6.7	147
	O K	4	7.9	250

*vincent.mauchamp@univ-poitiers.fr

[1] R. Egerton, *Electron Energy-Loss Spectroscopy in the Electron Microscope* (Plenum, New York, 1996).
[2] J. J. Rehr and R. C. Albers, Rev. Mod. Phys. **72**, 621 (2000).
[3] C. Hébert, Micron **38**, 12 (2007).
[4] M. S. Moreno, K. Jorissen, and J. J. Rehr, Micron **38**, 1 (2007).
[5] D. Cabaret, F. Mauri, and G. S. Henderson, Phys. Rev. B **75**, 184205 (2007).
[6] J. T. Titantah and D. Lamoen, Phys. Rev. B **70**, 075115 (2004).
[7] V. Mauchamp, T. Epicier, and J.-C. Le Bossé, Phys. Rev. B **77**, 235122 (2008).
[8] D. S. Su, C. Hébert, M. Willinger, and R. Schlögl, Micron **34**, 227 (2003).
[9] L. Calmels, C. Mirguet, and Y. Kihn, Phys. Rev. B **73**, 024207 (2006).
[10] F. Pailloux, M. Jublot, R. J. Gaboriaud, M. Jaouen, F. Paumier, and D. Imhoff, Phys. Rev. B **72**, 125425 (2005).
[11] R. O. Jones and O. Gunnarsson, Rev. Mod. Phys. **61**, 689 (1989).
[12] H. Kohl and H. Rose, Adv. Electron. Electron Phys. **65**, 173 (1985).
[13] B. L. Moiseiwitsch and S. J. Smith, Rev. Mod. Phys. **40**, 238 (1968).
[14] S. Doniach, P. M. Platzman, and J. T. Yue, Phys. Rev. B **4**, 3345 (1971).
[15] J. A. Soininen, A. L. Ankudinov, and J. J. Rehr, Phys. Rev. B **72**, 045136 (2005).
[16] D. K. Saldin and J. M. Yao, Phys. Rev. B **41**, 52 (1990).
[17] A. L. Ankudinov, B. Ravel, J. J. Rehr, and S. D. Conradson, Phys. Rev. B **58**, 7565 (1998).
[18] D. S. Su, H. W. Zandbergen, P. C. Tiemeijer, G. Kothleitner, M. Hävecker, C. Hébert, A. Knop-Gericke, B. H. Freitag, F. Hofer, and R. Schlögl, Micron **34**, 235 (2003).
[19] Y. Zhu, A. R. Moodenbaugh, G. Schneider, J. W. Davenport, T. Vogt, Q. Li, G. Gu, D. A. Fischer, and J. Tafto, Phys. Rev. Lett. **88**, 247002 (2002).
[20] S. Nufer, A. G. Marinopoulos, T. Gemming, C. Elsässer, W. Kurtz, S. Köstlmeier, and M. Rühle, Phys. Rev. Lett. **86**, 5066 (2001).
[21] J. A. Soininen and E. L. Shirley, Phys. Rev. B **64**, 165112 (2001).
[22] A. L. Ankudinov, Y. Takimoto, and J. J. Rehr, Phys. Rev. B **71**, 165110 (2005).
[23] I. Tanaka, H. Araki, M. Yoshiya, T. Mizoguchi, K. Ogasawara, and H. Adachi, Phys. Rev. B **60**, 4944 (1999).
[24] P. Moreau, F. Boucher, G. Goglio, D. Foy, V. Mauchamp, and G. Ouvrard, Phys. Rev. B **73**, 195111 (2006).
[25] M. Jaouen, G. Hug, B. Ravel, A. L. Ankudinov, and J. J. Rehr, Europhys. Lett. **49**, 343 (2000).
[26] N. Jiang and J. C. H. Spence, Phys. Rev. B **69**, 115112 (2004).
[27] G. Duscher, R. Buczko, S. J. Pennycook, and S. T. Pantelides, Ultramicroscopy **86**, 355 (2001).
[28] Z. Y. Wu, G. Ouvrard, P. Gressier, and C. R. Natoli, Phys. Rev. B **55**, 10382 (1997).
[29] L. V. Dobysheva, P. L. Potapov, and D. Schryvers, Phys. Rev. B **69**, 184404 (2004).
[30] V. Mauchamp, F. Boucher, G. Ouvrard, and P. Moreau, Phys. Rev. B **74**, 115106 (2006).
[31] E. Tamura, J. van Ek, M. Fröba, and J. Wong, Phys. Rev. Lett. **74**, 4899 (1995).
[32] J. Luitz, M. Maier, C. Hébert, P. Schattschneider, P. Blaha, K. Schwarz, and B. Jouffrey, Eur. Phys. J. B **21**, 363 (2001).
[33] S.-P. Gao, C. J. Pickard, M. C. Payne, J. Zhu, and J. Yuan, Phys. Rev. B **77**, 115122 (2008).
[34] A. J. Scott, R. Brydson, M. MacKenzie, and A. J. Craven, Phys. Rev. B **63**, 245105 (2001).
[35] T. Mizoguchi, I. Tanaka, M. Yoshiya, F. Oba, K. Ogasawara, and H. Adachi, Phys. Rev. B **61**, 2180 (2000).
[36] S.-D. Mo and W. Y. Ching, Phys. Rev. B **62**, 7901 (2000).
[37] C. Hébert, J. Luitz, and P. Schattschneider, Micron **34**, 219 (2003).
[38] F. M. F. de Groot, M. Grioni, J. C. Fuggle, J. Ghijsen, G. A. Sawatzky, and H. Petersen, Phys. Rev. B **40**, 5715 (1989).
[39] C. Elsässer and S. Köstlmeier, Ultramicroscopy **86**, 325 (2001).
[40] K. van Benthem, C. Elsässer, and M. Rühle, Ultramicroscopy **96**, 509 (2003).
[41] P. Blaha, K. Schwarz, G. Madsen, D. Kvaniscka, and J. Luitz, in *WIEN2k, An Augmented Plane Wave Plus Local Orbital Program for Calculating Crystal Properties*, edited by K. Schwarz (Technical Universität Wien, Austria, 2001).
[42] G. K. H. Madsen, P. Blaha, K. Schwarz, E. Sjöstedt, and L. Nordström, Phys. Rev. B **64**, 195134 (2001).
[43] E. Sjöstedt, L. Nordström, and D. J. Singh, Solid State Commun. **114**, 15 (2000).
[44] J. Desclaux, Comput. Phys. Commun. **1**, 216 (1970).
[45] J. Desclaux, Comput. Phys. Commun. **9**, 31 (1975).
[46] J. P. Perdew, K. Burke, and M. Ernzerhof, Phys. Rev. Lett. **77**, 3865 (1996).
[47] J. Korringa, Physica **13**, 392 (1947).
[48] W. Kohn and N. Rostoker, Phys. Rev. **94**, 1111 (1954).
[49] J. J. Kas, A. P. Sorini, M. P. Prange, L. W. Cambell, J. A. Soininen, and J. J. Rehr, Phys. Rev. B **76**, 195116 (2007).
[50] L. Hedin and S. Lundquist, in *Solid State Physics*, edited by F. Seitz, D. Turnbull, and H. Ehrenreic (Academic, New York, 1969), Vol. 23, p. 1.
[51] http://leonardo.phys.washington.edu/feff/
[52] L. Campbell, L. Hedin, J. J. Rehr, and W. Bardyszewski, Phys. Rev. B **65**, 064107 (2002).
[53] P. J. W. Weijs, M. T. Czyżyk, J. F. van Acker, W. Speier, J. B. Goedkoop, H. van Leuken, H. J. M. Hendrix, R. A. de Groot, G. van der Laan, K. H. J. Buschow, G. Wiech, and J. C. Fuggle, Phys. Rev. B **41**, 11899 (1990).
[54] J. Yuan, J. Electron Spectrosc. Relat. Phenom. **122**, 275 (2002).
[55] C. Heiliger, F. Heyroth, F. Syrowatka, H. S. Leipner, I. Maznichenko, K. Kokko, W. Hergert, and I. Mertig, Phys. Rev. B **73**, 045129 (2006).
[56] C. Cohen-Tannoudji, B. Diu, and F. Laloë, *Quantum Mechanics II* (Hermann, Paris, 1973).
[57] N. W. Ashcroft and N. D. Mermin, *Solid State Physics* (Brooks-Cole, Belmont, MA, 1976).
[58] Y. Joly, D. Cabaret, H. Renevier, and C. R. Natoli, Phys. Rev. Lett. **82**, 2398 (1999).
[59] P. Schattschneider, Ultramicroscopy **28**, 1 (1989).
[60] C. Ambrosch-Draxl and J. O. Sofo, Comput. Phys. Commun. **175**, 1 (2006).
[61] C. Lee and X. Gonze, Phys. Rev. B **49**, 14730 (1994).
[62] J. C. Slater, Phys. Rev. **36**, 57 (1930).
[63] S. Nufer, T. Gemming, C. Elsässer, S. Köstlmeier, and M. Rühle, Ultramicroscopy **86**, 339 (2001).

[64] E. Orhan, F. M. Pontes, C. D. Pinheiro, T. M. Boschi, E. R. Leite, P. S. Pizani, A. Beltrán, J. Andrés, J. A. Varela, and E. Longo, J. Solid State Chem. **177**, 3879 (2004).
[65] A. I. Nesvizhskii and J. J. Rehr, J. Synchrotron Radiat. **6**, 315 (1999).
[66] J. Schwitalla and H. Ebert, Phys. Rev. Lett. **80**, 4586 (1998).
[67] G. Onida, L. Reining, and A. Rubio, Rev. Mod. Phys. **74**, 601 (2002).